Important notice

Pre-subduction metasomatic enrichment of the oceanic lithosphere induced by plate flexure

S. PILET[1], N. ABE[2], L. ROCHAT[1], M.-A. KACZMAREK[1], N. HIRANO[3], S. MACHIDA[4], D. BUCHS[5], P.O. BAUMGARTNER[1] & O. MUNTENER[1].

[1] Institute of Earth Science, University of Lausanne, Switzerland;

[2] R&D Center for Ocean Drilling Science, Japan Agency for Marine-Earth Science and Technology (JAMSTEC), Yokosuka, Japan;

[3] Center for NE-Asian Studies, Tohoku University, Sendai, Japan;

[4] R&D Center for Submarine Resources, Japan Agency for Marine-Earth Science and technology (JAMSTEC), Yokosuka, Japan;

[5] School of Earth and Ocean Sciences, Cardiff University, UK.

Oceanic lithospheric mantle is generally interpreted as depleted mantle residue after mid ocean ridge basalt extraction. Several models have suggested that metasomatic processes can refertilize portions of the lithospheric mantle before subduction. Here, we report mantle xenocrysts and xenoliths in *petit-spot* lavas that provide direct evidence that the lower oceanic lithosphere is affected by metasomatic processes. Chemical similarity of clinopyroxene observed in *petit-spot* mantle xenoliths and clinopyroxene from melt-metasomatized garnet or spinel peridotites sampled by intracontinental basalts and kimberlites indicate that the metasomatic processes affecting oceanic and continental lithospheric mantle are similar. We suggest that extensional stresses in oceanic lithosphere such as plate bending in front of subduction zones allowing low degree melts from the seismic low velocity zone to percolate, interact, and weaken the oceanic lithospheric mantle indicating that percolation and metasomatism could be initiated by tectonic processes. Since plate flexure is a global mechanism in subduction zones, a significant portion of oceanic lithospheric mantle is likely to be metasomatized. Recycling of metasomatic domains into the convecting mantle is fundamental to understand the generation of small-scale mantle isotopic and volatile heterogeneities sampled by oceanic island and mid ocean ridge basalts.

The discovery of seafloor spreading and plate tectonics has suggested that oceanic lithospheric mantle represents the depleted residue after mid ocean ridge basalt (MORB) extraction. This hypothesis has been confirmed by the study of abyssal peridotites (e.g. ref. 1), yet several authors[2-4] have suggested that the oceanic lithospheric mantle could be re-enriched by metasomatic processes. To test whether oceanic lithospheric mantle is metasomatized is fundamental since studies of continental mantle xenoliths have demonstrated that metasomatic processes are intrinsically linked to the rheology, seismic properties and the chemical evolution of the continental lithospheric mantle[5]. It has been hypothesized that metasomatic enrichment of the oceanic lithospheric mantle could either be generated at the interface between the low-velocity zone and the base of the oceanic lithosphere[4] or by the percolation of low-degree melts produced in the periphery of mid ocean ridges but not collected to form MORB[3]. This later process is observed in (ultra-) slow spreading ridges where shallow oceanic lithospheric mantle is modified during incomplete MORB extraction and melt stagnation[6-9]. Metasomatic hydrous veins crosscutting peridotite observed in xenoliths sampled by ocean island basalts (OIB)[10-12] indicate that plume-lithosphere interaction could also modify the lithospheric mantle. However, direct evidence for metasomatic refertilization of the oceanic lithospheric mantle at a global scale is still missing. In this context, xenoliths/xenocrysts sampled by *petit-spot* lavas represents a unique opportunity to characterize the deep part of oceanic lithospheric mantle unaffected by mantle plume activity[13,14]. *Petit-spot* volcanoes represent small-volumes of magma and are interpreted as the products of deformation-driven melt segregation from the base of the lithosphere. Melt segregation could be related to plate flexure[13], but lithospheric deformation is also proposed as a mechanism to produce *petit-spot* volcanoes[15]. These small volcanoes have been originally discovered on the subducting Pacific plate east of Japan[13], yet several *petit-spot* localities have been identified from the Tonga[16], Chile[17], and Sunda trenches[18], or as an accreted *petit-spot* in Costa Rica[19], suggesting that *petit-spot* volcanism is a global process.

Metasomatic xenoliths and xenocrysts observed in petit-spot lava

The *petit-spot* lavas from Japan include various crustal and mantle xenoliths including gabbro, basalt, dolerite and peridotite[13,14]. Here, we report the presence of two mantle

xenoliths with clinopyroxene (cpx) trace-element compositions that differ significantly from the composition predicted for cpx in equilibrium with peridotite depleted by melt extraction at mid-ocean ridges (Fig. 1a). Both xenoliths show similar olivine, orthopyroxene (opx) and cpx major-element compositions (see supplementary information), but cpx trace-element compositions are different. The first xenolith (PSX1) contains cpx characterized by elevated light rare earth elements (LREE) / heavy rare earth elements (HREE) ratios and highly enriched incompatible trace-elements such as Th, U, Nb relative to cpx from depleted abyssal peridotite (Figs. 1a-1b). Cpx from the second xenolith (PSX2) shows similar incompatible trace-element enrichment, but no LREE/HREE fractionation (Figs. 1a-1c). The high magnesium number (molar Mg/Mg+Fe; Mg#: 91.8-92.4) and compositional homogeneity of these cpx exclude that their trace-element signature was related to re-equilibration of xenoliths with host melt during transport to the surface. Comparison of the trace-element patterns of Japanese *petit-spot* cpx (PSX1 and PSX2, Fig. 1) with cpx from xenoliths sampled in various tectonic settings (intra-continental, intra-oceanic, mid-ocean ridges, ophiolites) indicates that the incompatible trace-element content is characteristic of melt-metasomatized peridotite while the low HREE observed in xenolith PSX1 suggest equilibration with garnet. Co-existing orthopyroxene in xenolith PSX1 displays flat REE pattern supporting the hypothesis of equilibration with garnet, while opx from xenolith PSX2 is characterized by high HREE/LREE ratios typical of opx equilibrated in presence of spinel (*see supplementary information*). Assuming a geotherm of 50mW/m^2 for a 130 Ma year old lithospheric plate, equilibration conditions in the garnet stability field for PSX1 implies a minimum depth of ~70 km. This depth estimate corresponds to the deep part of the oceanic lithospheric mantle given that the base of the lithosphere has been imaged at 80 km and 73 km depth beneath Japan[20] and New Zealand[21] by seismic studies, respectively. Similarities between cpx trace-element signatures of the *petit-spot* xenoliths and melt-metasomatized garnet-peridotite xenoliths sampled by kimberlite from South-Africa[22] (Fig. 1c) or spinel-peridotite xenoliths from the East African Rift[23] (Fig. 1c) suggest that the metasomatic process affecting the oceanic or continental lithospheric mantle is similar. Clinopyroxene from both settings shows similar LREE/HREE fractionation and similar incompatible trace-element (Nb, Th, LREE) enrichments (Figs. 1b, 1c).

Mantle xenoliths and xenocrysts from continental settings demonstrate that cryptic metasomatism (i.e. diffusive exchange during porous flow) is generally associated to focused flow producing anhydrous and hydrous cumulates/veins[24,25]. Evidence for the formation of metasomatic veins in oceanic lithosphere is preserved in cpx xenocrysts from alkaline sills interpreted as an accreted *petit-spot* in northern Costa-Rica[19]. These ~175 Ma sills interlayered with radiolarite are interpreted as the basal part of intraplate volcanoes accreted along the west central America margin[19]. These alkaline sills show compositional features similar to the *petit-spot* lavas from Japan (i.e. high K_2O/Na_2O ratios, similar trace element patterns) supporting similar petrogenetic processes[19]. The Costa Rica *petit-spot* sills were not necessarily associated to plate flexure but more likely related to tectonic stresses associate to the early stages of the Pacific plate formation[19]. Costa Rica sills are porphyric, host large zoned cpx phenocrysts that occasionally contain green cores. These green-core cpx (GCPX) are interpreted as xenocrysts based on their low Mg#, high Al/Ti ratios and high Na_2O contents compared to the surrounding rims in equilibrium with the basaltic host-lavas (Fig. 2a-2c). Such evolved compositions suggest crystallization from differentiated liquids at lithospheric conditions. But the main argument supporting the interpretation of GCPX as relic of metasomatic veins is their composition similar to cpx observed in metasomatic veins from the French Pyrenees and in mantle xenoliths from Canary Islands[11] (Fig. 2). The presence of melt-metasomatized peridotite and GCPX in Japanese and Costa Rican *petit-spot* lavas provides direct evidence that porous and focused metasomatic flow affect deep parts of the oceanic lithosphere.

Potential origin of the metasomatic imprint

It is fundamental to determine if metasomatic domains are inherited from the formation of oceanic lithosphere or if metasomatism affects the lithosphere long after its formation at mid oceanic ridges. The presence of relic of subcontinental lithospheric mantle (SCLM) blobs in the oceanic lithospheric mantle has been suggested to explain metasomatism observed in Cape Verde xenoliths[26] for example. However, much of the Pacific plate is produced in an intermediate to fast spreading setting far from continental crust. To incorporate SCLM domains in Pacific lithosphere requires that these domains have travelled thousands of kilometers from their original location

making this hypothesis difficult to maintain. In addition the different trace element patterns of cpx in *petit-spot* xenoliths suggest that the metasomatic process affect peridotites at different depths in the spinel and garnet stability field, which seems difficult to reconcile with the incorporation of metasomatized SCLM within the Pacific oceanic lithospheric mantle. We prefer the hypothesis that the percolation of low-degree melts extracted from the base of the lithosphere explains the metasomatic imprint observed in *petit-spot* xenoliths/xenocrysts.

The high variability of trace-element patterns of the metasomatized cpx from garnet-peridotite from South Africa (Fig. 1b) or from East Africa Rift (Fig. 1c) have both been interpreted as related to "chromatographic" effects associated to the percolation of low degree volatile-rich silicate melts migrating in depleted peridotite[22,23,27], but the origin of these low degree melts is debated. For example, this metasomatic melt has been linked to Group-1 kimberlite for the case of south Africa[22] while plume-derived melts have been proposed for the case of the East African Rift[23]. Seismic imaging of the top parts of the northwestern pacific plate[28] does not show any signs of mantle plumes during the evolution of the oceanic plate in the area where Japanese petit-spot volcanoes were found. In the absence of mantle plumes, and assuming that plate flexure associated to petit-spot genesis does not generate any pressure - temperature variation able to initiate mantle melting[13-15], the low velocity zone (LVZ) is the only potential source of melts beneath the oceanic lithosphere[14,29]. Reduced shear wave velocities at the base of the oceanic lithosphere were interpreted as partially molten asthenosphere consisting of horizontal melt-rich layers embedded in an otherwise melt-free mantle[20]. Low degree volatile-rich melts ($F \approx 0.035 - 2\%$) have been also inferred at the base of the oceanic lithosphere in order to explain the physical properties of the LVZ[20,30-32], but the carbonatitic[30] or silicate[32] nature of these melts is still in debate. The cpx trace-element patterns reported in figure 1 indicate the percolation of silicate melts rather than carbonatites, as the percolation of carbonatitic melts is expected to produce Nb, Zr and Hf negative anomalies (Fig. 2). The low permeability of the lithospheric mantle and liquid-solid surface tension limits the potential passive extraction of small melt fractions from the LVZ and its percolation across the lithosphere[33-36]. Passive melt migration seems, therefore, difficult to reconcile with melt percolation on large distance (~10-20 km) require to explain the metasomatic enrichment observed in *petit-spot* grt and spl-peridotite xenoliths. The location of Japanese *petit-spot* volcanoes and the age

progression of the lavas in the direction opposite to that of plate motion have clearly established a link between tectonic stress, i.e. plate flexure, and the extraction of silicate melts associated to *petit-spot* genesis[13-15,29]. We suggest that metasomatic enrichment recorded by petit-spot xenoliths / xenocrysts is associated to a similar process. But, in contrast to models which propose the extraction of *petit-spot* melt from the LVZ via the development of deep lithospheric cracks[13,14], the chemical signature of *petit-spot* xenoliths/xenocrysts indicate interaction with the lithospheric mantle. We propose that (I) extensional processes related to plate flexure and/or lithospheric stress allow this low degree melts to percolate and differentiate across the oceanic lithospheric mantle thereby producing (II) refertilization of the depleted peridotites, (III) the formation of metasomatic veins, and in some cases (IV) the eruption of *petit-spot* lavas at the surface (Fig. 3). To test this interpretation, we developed a forward model to determine the cpx trace elements patterns produced during porous and focused flow linked to the percolation of LVZ melts. The trace-element fractionation during melt percolation in a peridotite column is simulated using the numerical "plate" model[37] assuming that the composition of the melts extracted from the LVZ was similar to *petit-spot* melts (*see supplementary information for model parameters*) (Figs. 4b-4c). Results indicate that after a few meters of porous melt flow and reaction with peridotite, the initial cpx HREE contents remain unmodified while the highly incompatible elements such as Th, U, or La are strongly modified by the reacting melt. Our models show that cpx trace-element patterns of xenoliths PSX1 and PSX2 can be reproduced by the percolation of *petit-spot* melts through peridotite at different depths. This indicates that the incompatible trace-element pattern of cpx from metasomatized peridotite is controlled by "chromatographic" effects rather than by the initial composition of the percolating melt (see supplementary information). In contrast, the general trace-element enrichment in minerals from metasomatic cumulates is directly related to the evolution of the metasomatic melt during focused melt flow (Figs. 4d-4e). The evolution of mineral and melt compositions during fractional crystallization in metasomatic veins is calculated using a similar approach as reported by Pilet *et al.* (ref. [38]). The trace-element pattern of GCPX type 1 observed in Costa Rica *petit-spot* lavas could be explained by the formation of anhydrous and hydrous cumulates, while the concave downward shape for REE and the positive Zr, Hf anomalies observed in GCPX type 2 require the additional fractionation of accessory phases, such as apatite, allanite and rutile (Figs. 4d-4e),

phases which are observed in metasomatic veins crosscutting lithospheric mantle. This forward geochemical model confirms that percolation of low degree volatile-rich melts across the oceanic lithospheric mantle could explain the chemical signature of metasomatized xenoliths and xenocrysts sampled by *petit-spot* lavas and points out the importance of the fractionation of hydrous cumulates within the lithospheric mantle to produce the trace element patterns of GCPX xenocrysts (Fig. 2 and Fig. S8).

Implications for the nature of the oceanic lithospheric mantle

The discovery of metasomatized xenoliths/xenocrysts extracted from the base of the Pacific plate has fundamental implications for our understanding of metasomatic processes at the lithosphere – asthenosphere boundary and on the nature of subducted oceanic lithosphere. First, our data indicate that the base of the oceanic lithosphere does not represent an impermeable barrier for melt percolation as commonly assumed. Metasomatic imprints recorded in grt- and spl- peridotite *petit-spot* xenoliths demonstrate that lithospheric extension allowed low degree asthenospheric melts to percolate and interact with overlying lithospheric mantle. This is consistent with theoretical and experimental studies indicating that deformation is critical for melt percolation and extraction of low-melt fractions (e.g. refs 33-35).

Second, metasomatism by small-melt fractions has been classically restricted to continental lithospheric mantle[5,22,23,25] or to the oceanic mantle affected by a mantle plume[11,12], the discovery of melt-metasomatized peridotites and relic of metasomatic veins in *petit-spot* lavas call for a general mechanism at the lithosphere-asthenosphere boundary. The link between lithosphere deformation and initiation of melt percolation indicates that metasomatic processes are not necessarily related to passive or active upwelling (i.e. mid ocean ridges or mantle plume), but could be initiated by tectonic processes. The cases studies from Japan[13] and Costa Rica[19] indicate that melt percolation and metasomatism can be generated by deformation processes in the deep oceanic lithosphere and are also likely in other tectonic settings such as rifted margins or back-arc initiation. This aspect is important for the geodynamic and geophysical processes at the lithosphere-asthenosphere boundary as percolation and differentiation of low degree melts will modify the rheology (melt-related weakening) and the seismic and electric properties of the lithospheric mantle[39-41].

The last implication of our study is related to the formation of chemical mantle heterogeneities. Recycling and long-term storage of oceanic lithosphere (mantle and crust) into the convecting mantle is the most common mechanism proposed to explain the compositional and isotopic heterogeneity of the Earth mantle. Recycling of the depleted oceanic lithosphere through time is expected to produce the DMM mantle component, but several authors suggest that metasomatism / refertilization could modify the isotopic evolution of oceanic lithospheric mantle after recycling into the convecting mantle[2-4,42]. Our findings provide direct evidence that oceanic lithospheric mantle is metasomatized before being recycled into the convecting mantle, but to constrain what fraction of the oceanic lithosphere is affected is more difficult to estimate. Different arguments suggests that even metasomatic enrichment of the lithosphere is limited to specific zones, this process is critical to understand the global mantle circle. First, geothermobarometry on Japanese *petit-spot* mantle xenoliths have revealed a geotherm much hotter than expected for a ca. 130 Ma old seafloor[14]. Yamamoto and co-authors (ref. 14) interpret these highly localized thermal anomalies as associated to *petit-spot* melt extraction, yet the production of such thermal anomalies requires a higher melt fraction percolating the mantle lithosphere than presently observed at the surface. They conclude that *petit-spot* volcanoes just represent "the tip of the iceberg" and significantly more melt could be trapped within the lithosphere[14]. Second, topographic rises of a few hundred meters of the downgoing plates are observed in most subduction zones (e.g. ref. 43) and *petit-spot* volcanoes have been detected in several places[13,16-19]. This suggests that plate bending and its associated volcanism/metasomatism is a global mechanism. Third, geochemical simulations indicate that the volume of impregnated mantle and metasomatic veins does not need to be large to affect the isotopic evolution of the recycled lithospheric mantle[38]. The cpx compositions of the *petit-spot* xenoliths and xenocrysts (Figs. 1 and 2) confirm trace element models of metasomatic enrichment in oceanic lithosphere[38] indicating that the incompatible trace-element budget of oceanic lithospheric mantle, including Rb/Sr, Sm/Nd and U/Pb ratios controlling the evolution of radiogenic isotopic systems, is substantially modified by the percolation and differentiation of low-degree "wet" melts. Monte Carlo simulations of metasomatic enrichment[38] indicate that recycling of lithospheric mantle containing only 1% of metasomatic domains could produce isotopic compositions ranging from depleted MORB mantle (DMM) to high μ (HIMU, i.e. high

$^{238}U/^{204}Pb$ (=μ) ratio) mantle end-members after 1.5 Ga of isolation and chemical diffusion[38]. It is therefore reasonable to assume that a significant portion of oceanic lithospheric mantle is affected by metasomatism before being recycled into the convecting mantle. Such metasomatic processes could also modify the volatile content of the lithospheric mantle as demonstrated by the study of garnet-pyroxenites from Hawaii [12]. The composition of the oceanic lithospheric mantle is thus unlikely to be universally depleted, but could integrate enriched domains which could, after recycling and storage into the convecting mantle, produce some of the isotopically and volatile enriched components observed in the source of OIBs or MORBs[2-4,12,38].

References

1 Johnson, K. T. M., Dick, H. J. B. & Shimizu, N. Melting in the Oceanic Upper Mantle - an Ion Microprobe Study of Diopsides in Abyssal Peridotites. *Journal of Geophysical Research-Solid Earth* **95**, 2661-2678 (1990).

2 Hanson, G. N. Geochemical evolution of the suboceanic mantle. *Journal of the Geological Society of London* **134**, 235-253 (1977).

3 Halliday, A. N. *et al.* Incompatible Trace-Elements in Oib and Morb and Source Enrichment in the Sub-Oceanic Mantle. *Earth and Planetary Science Letters* **133**, 379-395 (1995).

4 Niu, Y. L. & O'Hara, M. J. Origin of ocean island basalts: A new perspective from petrology, geochemistry, and mineral physics considerations. *Journal of Geophysical Research-Solid Earth* **108**, doi:10.1029/2002JB002048 (2003).

5 Griffin, W. L., O'Reilly, S. Y., Afonso, J. C. & Begg, G. C. The Composition and Evolution of Lithospheric Mantle: a Re-evaluation and its Tectonic Implications. *Journal of Petrology* **50**, 1185-1204 (2009).

6 Seyler, M., Toplis, M. J., Lorand, J. P., Luguet, A. & Cannat, M. Clinopyroxene microtextures reveal incompletely extracted melts in abyssal peridotites. *Geology* **29**, 155-158 (2001).

7 Warren, J. M. & Shimizu, N. Cryptic Variations in Abyssal Peridotite Compositions: Evidence for Shallow-level Melt Infiltration in the Oceanic Lithosphere. *Journal of Petrology* **51**, 395-423 (2010).

8 Dick, H. J. B., Lissenberg, J. C. & Warren, J. M. Mantle Melting, Melt Transport, and Delivery Beneath a Slow-Spreading Ridge: The Paleo-MAR from 23° 15′ N to 23 ° 45′ N. *Journal of Petrology* **51**, 425-467 (2010).

9 Muntener, O., Pettke, T., Desmurs, L., Meier, M. & Schaltegger, U. Refertilization of mantle peridotite in embryonic ocean basins: trace element and Nd isotopic evidence and implications for crust-mantle relationships. *Earth and Planetary Science Letters* **221**, 293-308 (2004).

10 Roden, M. K., Hart, S. R., Frey, F. A. & Melson, W. G. Sr, N and Pb isotopic and REE geochemistry of St. Paul's rocks: the metamorphic and metasomatic development of an alkali basalt mantle source. *Contributions to Mineralogy and Petrology* **85**, 376-390 (1984).
11 Wulff-Pedersen, E., Neumann, E. R., Vannucci, R., Bottazzi, P. & Ottolini, L. Silicic melts produced by reaction between peridotite and infiltrating basaltic melts: ion probe data on glasses and minerals in veined xenoliths from La Palma, Canary Islands. *Contributions to Mineralogy and Petrology* **137**, 59-82 (1999).
12 Bizimis, M. & Peslier, A. H. Water in Hawaiian garnet pyroxenites: Implications for water heterogeneity in the mantle. *Chemical Geology* **397**, 61-75 (2015).
13 Hirano, N. *et al.* Volcanism in response to plate flexure. *Science* **313**, 1426-1428 (2006).
14 Yamamoto, J., Korenaga, J., Hirano, N. & Kagi, H. Melt-rich lithosphere-asthenosphere boundary inferred from petit-spot volcanoes. *Geology* **42**, 967-970 (2014).
15 Valentine, G. A. & Hirano, N. Mechanisms of low-flux intraplate volcanic fields-Basin and Range (North America) and northwest Pacific Ocean. *Geology* **38**, 55-58 (2010).
16 Hirano, N., Koppers, A. A. P., Takahashi, A., Fujiwara, T. & Nakanishi, M. Seamounts, knolls and petit spot monogenetic volcanoes on the subducting Pacific Plate. *Basin Research* **20**, 543-553 (2008).
17 Hirano, N. *et al.* Petit-spot lava fields off the central Chile trench induced by plate flexure. *Geochemical Journal* **47**, 249-257 (2013).
18 Taneja, R. *et al.* $^{40}Ar/^{39}Ar$ geochronology and the paleoposition of Christmas Island (Australia), Northeast Indian Ocean. *Gondwana Research* **28**, 391-406 (2015).
19 Buchs, D. M. *et al.* Low-volume intraplate volcanism in the Early/Middle Jurassic Pacific basin documented by accreted sequences in Costa Rica. *Geochemistry Geophysics Geosystems* **14**, 1552-1568 (2013).
20 Kawakatsu, H. *et al.* Seismic evidence for sharp lithosphere asthenosphere boundaries of oceanic plates. *Science* **324**, 499-502 (2009).
21 Stern, T. A. *et al.* A seismic reflection image for the base of a tectonic plate. *Nature* **518**, 85-88 (2015).
22 Gregoire, M., Bell, D. R. & Le Roex, A. P. Garnet lherzolites from the Kaapvaal craton (South Africa): Trace element evidence for a metasomatic history. *Journal of Petrology* **44**, 629-657 (2003).
23 Bedini, R. M., Bodinier, J. L., Dautria, J. M. & Morten, L. Evolution of LILE-enriched small melt fractions in the lithospheric mantle: a case study from the East African Rift. *Earth and Planetary Science Letters* **153**, 67-83 (1997).
24 Wilshire, H. G. in *Mantle metasomatism and alkaline magmatism* Vol. 215 (eds E.M. Morris & J.D. Pasteris) 47-60 (Geological Society of America Special Paper, 1987).
25 Harte, B., Hunter, R. H. & Kinny, P. D. Melt geometry, movement and crystallization, in relation to mantle dykes, veins and metasomatism. *Philosophical transactions of the Royal Society of London Serie A -Math. Phys. Eng. Sci.* **342**, 1-21 (1993).
26 Bonadiman, C., Beccaluva, L., Coltorti, M. & Siena, F. Kimberlite-like metasomatism and 'Garnet signature' in spinel-peridotite xenoliths from Sal,

Cape Verde archipelago: Relics of a subcontinental mantle domain within the Atlantic oceanic lithosphere? *Journal of Petrology* **46**, 2465-2493 (2005).

27 Navon, O. & Stolper, E. Geochemical consequence of melt percolation: the upper mantle as a chromatographic column. *Journal of Geology* **95**, 285 - 307 (1987).

28 Kodaira, S. *et al.* Seismological evidence of mantle flow driving plate motions at a palaeo-spreading centre. *Nature Geoscience* **7**, 371-375 (2014).

29 Machida, S. *et al.* Petit-spot geology reveals melts in upper-most asthenosphere dragged by lithosphere. *Earth and Planetary Science Letters* **426**, 267-279 (2015).

30 Gaillard, F., Malki, M., Iacono-Marziano, G., Pichavant, M. & Scaillet, B. Carbonatite Melts and Electrical Conductivity in the Asthenosphere. *Science* **322**, 1363-1365 (2008).

31 Hirschmann, M. M. Partial melt in the oceanic low velocity zone. *Physics of the Earth and Planetary Interiors* **179**, 60-71 (2010).

32 Ni, H. W., Keppler, H. & Behrens, H. Electrical conductivity of hydrous basaltic melts: implications for partial melting in the upper mantle. *Contributions to Mineralogy and Petrology* **162**, 637-650 (2011).

33 Katz, R. F., Spiegelman, M. & Holtzman, B. The dynamics of melt and shear localization in partially molten aggregates. *Nature* **442**, 676-679 (2006).

34 Kohlstedt, D. L. & Holtzman, B. K. Shearing melt out of the Earth: An experimentalist's perspective on the influence of deformation on melt extraction. *Annual Review of Earth and Planetary Sciences* **37**, 561-593 (2009).

35 Holtzman, B. K. Questions on the existence, persistence, and mechanical effects of a very small melt fraction in the asthenosphere. *Geochem. Geophys. Geosyst.* **17**, 470–484 (2016).

36 Pec, M., Holtzman, B. K., Zimmerman, M. & Kohlstedt, D. L. Reaction infiltration instabilities in experiments on partially molten mantle rocks. *Geology* **43**, 575-578 (2015).

37 Vernieres, J., Godard, M. & Bodinier, J. L. A plate model for the simulation of trace element fractionation during partial melting and magma transport in the Earth's upper mantle. *Journal of Geophysical Research-Solid Earth* **102**, 24771-24784, (1997).

38 Pilet, S., Baker, M. B., Muntener, O. & Stolper, E. M. Monte Carlo Simulations of Metasomatic Enrichment in the Lithosphere and Implications for the Source of Alkaline Basalts. *Journal of Petrology* **52**, 1415-1442 (2011).

39 Yang, X. Z. & McCammon, C. Fe3+-rich augite and high electrical conductivity in the deep lithosphere. *Geology* **40**, 131-134 (2012).

40 Rader, E. *et al.* Characterization and petrological constraints of the midlithospheric discontinuity. *Geochem. Geophys. Geosyst.* **16**, 3484–3504 (2015).

41 Selway, K., Ford, H. & Kelemen, P. The seismic mid-lithosphere discontinuity. *Earth and Planetary Science Letters* **414**, 45-57 (2015).

42 Pilet, S., Hernandez, J., Sylvester, P. & Poujol, M. The metasomatic alternative for ocean island basalt chemical heterogeneity. *Earth and Planetary Sciences Letter* **236**, 148-166 (2005).

43 Watts, A. B. & Talwani, M. Gravity anomalies seaward of deep-sea trenches and their tectonic implications. *Geophysical Journal of the Royal Astronomical Society* **36**, 57-90 (1974).

44 McDonough, W. F. & Sun, S. S. The Composition of the Earth. *Chemical Geology* **120**, 223-253 (1995).

Acknowledgements

This work benefited from discussions with Michael. M. Baker, Daniela Rubatto and Jolante van Wijk. This work is supported by the Swiss National Science Foundation, grant 200021_140494 (S.P.) and by the Toray Science Foundation, Toray science and technology grant #11–5208 (N.H.).

Author Contributions

S.P. and N.A designed the study. *Petit-spot* samples from Japan and Costa Rica were collected by N.H., N.A., and S.M. and by D.B., P.B., L. R., and S.P. respectively. L.R., S.P., N.A. performed the EMPA and LA-ICP-MS measurements. M-A. K. and S.P. conducted the porous and focused flow numerical simulations. All authors discussed the results and their implications. S.P., L.R., O.M., M-A. K., and D.B. wrote the text. All authors reviewed and approved the manuscript.

Additional information

Supplementary Information is linked to the online version of the paper

Competing financial interests

The authors declare no competing financial interests.

Figure Captions

Figure 1. Clinopyroxene composition normalized to Primitive Mantle for Japanese *petit-spot* peridotite xenolith compared to abyssal or melt-metasomatized continental peridotites. a Clinopyroxene from Japanese *petit-spot* peridotite xenolith PSX1 and PSX2 compared to individual clinopyroxene composition from melt-metasomatized and residual abyssal peridotite from the Atlantis II fracture Zone on the Southwest Indian Ridge[7]. **b** Clinopyroxene from Japanese PSX1 compared to cpx composition from melt-metasomatized garnet-peridotite from South Africa[22]. **c** Clinopyroxene from Japanese PSX2 compared to clinopyroxene composition from melt-metasomatized spinel-peridotite from East African Rift [23]. The clinopyroxene range for abyssal peridotites[1] is shown in all panels

as reference (grey area). Trace-element contents are normalized to primitive mantle values from ref. 44.

Figure 2. Comparison of clinopyroxene xenocrysts composition from Costa Rica *petit-spot* sills with cpx from lithospheric metasomatic veins. a-b major-element composition of clinopyroxene from Costa Rica petit-spot sills (**a**), and metasomatic veins from the French Pyrenees and La Palma (Canary Islands)[11] (**b**) reported in a portion of the pyroxene quadrilateral. **c**, Transmitted light image of a green-core clinopyroxene surrounding by a rim in equilibrium with host alkaline lava (Costa Rica). **d**, Metasomatic veins crosscutting peridotite (picture from Avezac mantle outcrop, French Pyrenees). **e-f**, Trace-element contents normalized on primitive mantle diagrams (value from ref. 44) for clinopyroxene from Costa Rica alkaline sills (**e**), from metasomatic veins from French Pyrenees and La Palma (Canary Islands)[11] (**f**).

Figure 3. Schematic model illustrating the metasomatism of the oceanic lithospheric mantle associated to plate flexure. (I) Extension at the base of the lithosphere created by plate flexure allows low degree melts present at the top of the asthenosphere to percolate into the lithospheric mantle. The percolation and differentiation of these melts produce various (an-) hydrous metasomatic veins and/or cumulates as a function of pressure and temperature, and cryptic metasomatism in oceanic lithosphere (II-III). (IV) In some cases, the reacting low degree melts could reach the surface and generate the *petit-spot* sills and lavas. (V) Recycling and storage of oceanic lithosphere into the convecting mantle containing incompatible element enriched metasomatized domains could produce some of the isotopically enriched components observed in the source of MORBs or OIBs.

Figure 4. Forward modeling of metasomatic enrichment of the oceanic lithospheric mantle. a, Schematic model illustrating focused and porous melt flow processes associated with the formation of metasomatic cumulates and cryptic metasomatism in peridotite. The composition of the low degree melt is assumed to be similar to *petit-spot* lava composition from Japan[13], and f is the melt fraction at different stages of differentiation. **b-c**, For the cryptic metasomatic enrichment, the chromatographic effect is calculated using the numerical "Plate model"[37] with the

percolation of *petit-spot* melt across a slightly depleted peridotite in spinel and garnet facies, respectively. Panel **b** represents clinopyroxene from PSX1 and panel **c** clinopyroxene from PSX2 compared to clinopyroxene patterns predicted by numerical modeling. The clinopyroxene calculated in step 1 (dark green line), and from 10 to 50 (lighter green colors lines) of the porous flow plate model are shown. **d-e,** Green-core clinopyroxene xenocrysts (GCPX) from Costa Rica *petit-spot* sills as a function of their trace element signature (GCPX type 1 and 2) compared to model-generated clinopyroxene from anhydrous (blue lines) and hydrous cumulates (orange to red lines). The focused melt flow model is calculated using the approach described by Pilet *et al.* [38]. The model indicates that the different trace element patterns of GCPX could be explained by the difference of accessory phases (rutile, apatite, sphene, allanite), which crystallized during focused melt flow. Trace-element contents are normalized to primitive mantle values from ref. [44]. Notes: ol: olivine, amph: amphibole, Grt: garnet, plg: plagioclase, rut: rutile. *See supplementary information for the modeling parameters*.

Methods

Wavelength-dispersive electron microprobe analyses of Japanese xenoliths minerals, Costa Rica cpx xenocrysts and cpx from French Pyrenees metasomatic veins were obtained at University of Lausanne using a JEOL JXA-8200 (5 spectrometers) electron probe microanalyzer. A 15 KeV accelerating voltage was used for all analyses. Olivine (ol), orthopyroxene (opx) and clinopyroxene (cpx) were analyzed with a 20 nA focused beam (~1 μ m). All data were processed using CITZAF [45]. Cpx, opx, and ol representative analyses are reported in Table S1 and Table S2 for Japanese xenoliths, while Costa Rica cpx xenocrysts and cpx from French Pyrenees metasomatic veins analyses are reported in Table S3.

Concentrations of trace elements (REE, HFSE and LILE) in cpx and opx were determined in situ on polished thick-sections (~80µm) for green-core cpx from Costa Rica sills or on polished EPMA thin- sections (30µm) for petit-spot xenoliths using Laser Ablation Inductively Coupled Plasma Mass Spectrometry (LA-ICP-MS) techniques at the Institute of Earth Sciences, University of Lausanne, Switzerland.

Two distinct LA-ICP-MS systems were used during this study. The relatively small size of cpx of xenolith 017c (PSX1) and the presence of fractures an/or inclusions require a high spatial resolution. So, we performed these analyses using a Thermo Scientific Element XR sector-field ICP-MS coupled to NewWave UP-193 (193 nm) ArF excimer ablation system that provides higher sensibility and allowed to perform analyses using 15-20 μm spot size. Analyses were acquired using an energy density of ~5.0 J/cm^2 and a pulse repetition rate of 12 Hz. Acquisition time: the gas blank was measured during ~ 120s before firing the laser, the minerals were analyzed for ~ 20 to 40s as a function of the thickness of the thin section. The standard glass NIST glass 612 was analyzed two times at the beginning and two times at the end of each series with a diameter of 75μm. Similar conditions, excepted the spot size (75 μm), were used to measure trace elements content in opx from xenoliths 017c (PSX1) and 001-2 (PSX2).

Analyses on the xenolith 001-2 (PSX2) and cpx from Costa-Rican petit-spot sills and French Pyrenees metasomatic veins were performed on a quadrupole spectrometer Agilent 7700 interfaced to a GeoLas 200M (193 nm) ArF excimer ablation system at an energy density of ~16 J/cm^2 and pulse repetition rate of 8 Hz. A spot size of 120 μm was used for glass standard analyses, while the spot size for analyses varied from 40 μm to 80 μm depending on the presence of fractures or inclusions in the minerals.

All data were reduced using CONVERT and LAMTRACE software[46]. NIST SRM-612 glass was used as an external standard and the CaO content of cpx or SiO_2 content of opx (from electron microprobe measurements) served as an internal standard. Cpx and opx data are reported in Table S1 and Table S2 for Japanese xenoliths PSX1 and PSX2 respectively while the trace element content of Costa Rica cpx xenocrysts (GCPX) and cpx from the French Pyrenees metasomatic veins was reported in Table S3

Additional information about the sample description, discussion about the parameters used in the models shown in fig. 4, and data supporting the finding of this study are available in the supplementary information file.

References

45 Armstrong, J. T. in *Microbeam Analysis* (ed D.E. Newbury) 239-246 (San Francisco Press, 1988).

46 Longerich, H. P., Jackson, S. E. & Gunther, D. Laser ablation inductively coupled plasma mass spectrometric transient signal data acquisition and analyte concentration calculation. *Journal of Analytical Atomic Spectrometry* **11**, 899-904 (1996).

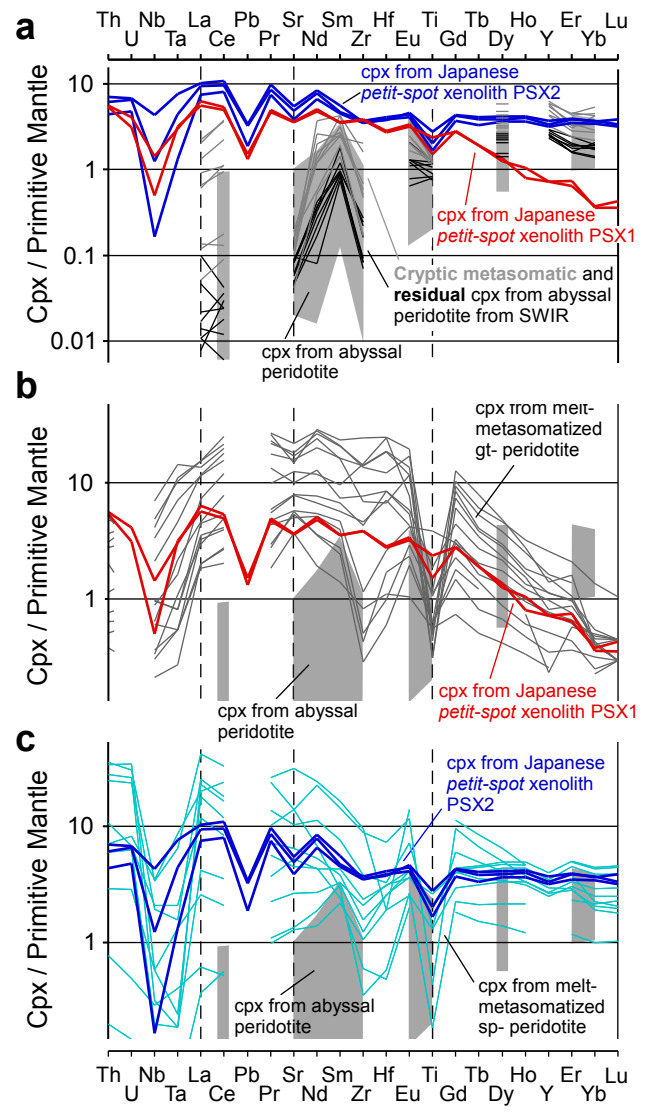
a
Th Nb La Pb Sr Sm Hf Ti Tb Ho Er Lu
U Ta Ce Pr Nd Zr Eu Gd Dy Y Yb
Cpx / Primitive Mantle
10
1
0.1
0.01
cpx from Japanese
petit-spot xenolith PSX2
cpx from Japanese
petit-spot xenolith PSX1
Cryptic metasomatic and
residual cpx from abyssal
peridotite from SWIR
cpx from abyssal
peridotite
b
Cpx / Primitive Mantle
10
1
cpx from melt-
metasomatized
gt- peridotite
cpx from Japanese
petit-spot xenolith PSX1
cpx from abyssal
peridotite
c
Cpx / Primitive Mantle
10
1
cpx from Japanese
petit-spot xenolith
PSX2
cpx from abyssal
peridotite
cpx from melt-
metasomatized
sp- peridotite
Th Nb La Pb Sr Sm Hf Ti Tb Ho Er Lu
U Ta Ce Pr Nd Zr Eu Gd Dy Y Yb

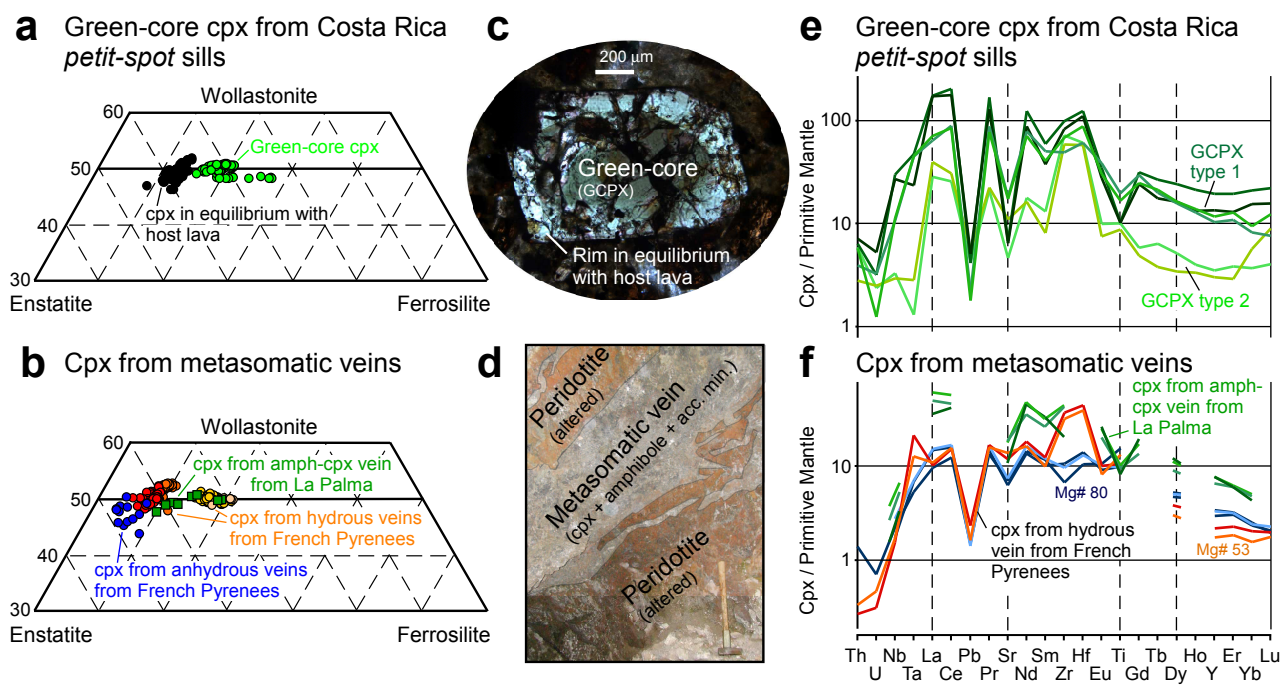
a
Green-core cpx from Costa Rica
petit-spot sills
Wollastonite
60
50
40
30
Green-core cpx
cpx in equilibrium with
host lava
Enstatite
Ferrosilite
b
Cpx from metasomatic veins
Wollastonite
60
50
40
30
cpx from amph-cpx vein
from La Palma
cpx from hydrous veins
from French Pyrenees
cpx from anhydrous veins
from French Pyrenees
Enstatite
Ferrosilite
c
200 µm
Green-core
(GCPX)
Rim in equilibrium
with host lava
d
Peridotite
(altered)
Metasomatic vein
(cpx + amphibole + acc. min.)
Peridotite
(altered)
e
Green-core cpx from Costa Rica
petit-spot sills
Cpx / Primitive Mantle
100
10
1
GCPX
type 1
GCPX type 2
f
Cpx from metasomatic veins
Cpx / Primitive Mantle
10
1
cpx from amph-
cpx vein from
La Palma
Mg# 80
cpx from hydrous
vein from French
Pyrenees
Mg# 53
Th Nb La Pb Sr Sm Hf Ti Tb Ho Er Lu
U Ta Ce Pr Nd Zr Eu Gd Dy Y Yb

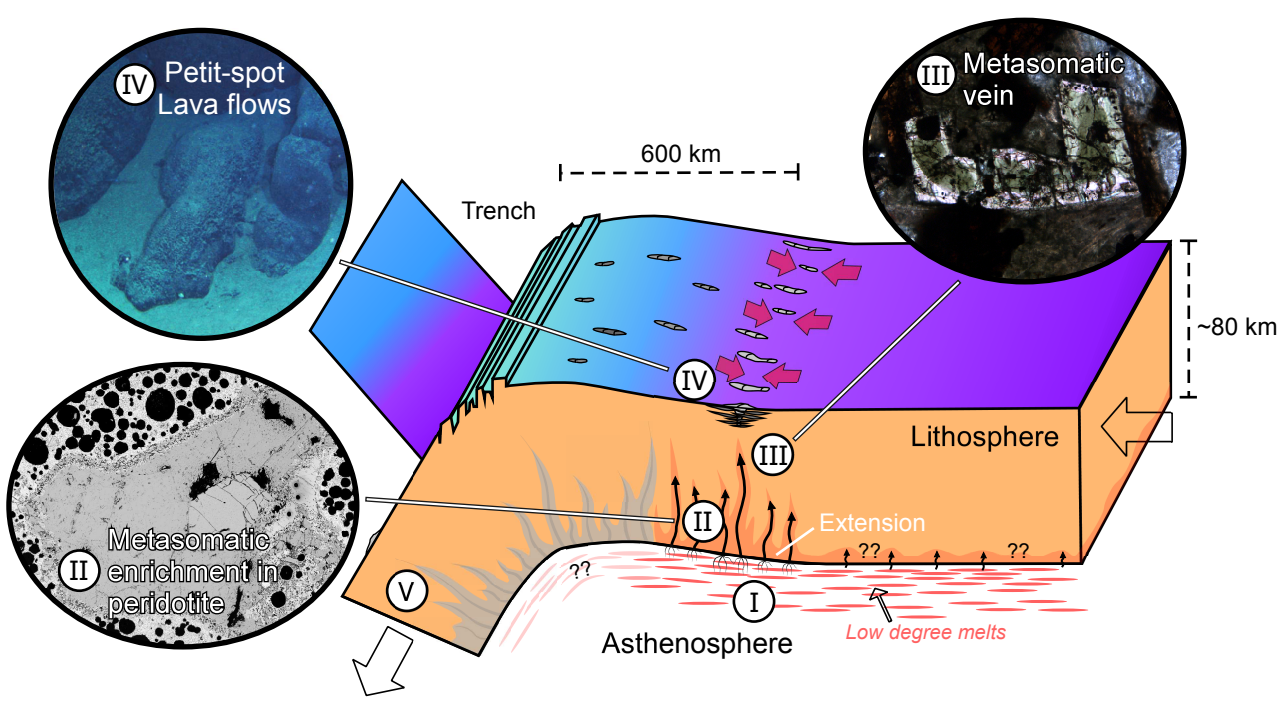
IV
Petit-spot
Lava flows
III
Metasomatic
vein
600 km
Trench
~80 km
IV
Lithosphere
III
II
Extension
??
??
??
V
I
Asthenosphere
Low degree melts
II
Metasomatic
enrichment in
peridotite

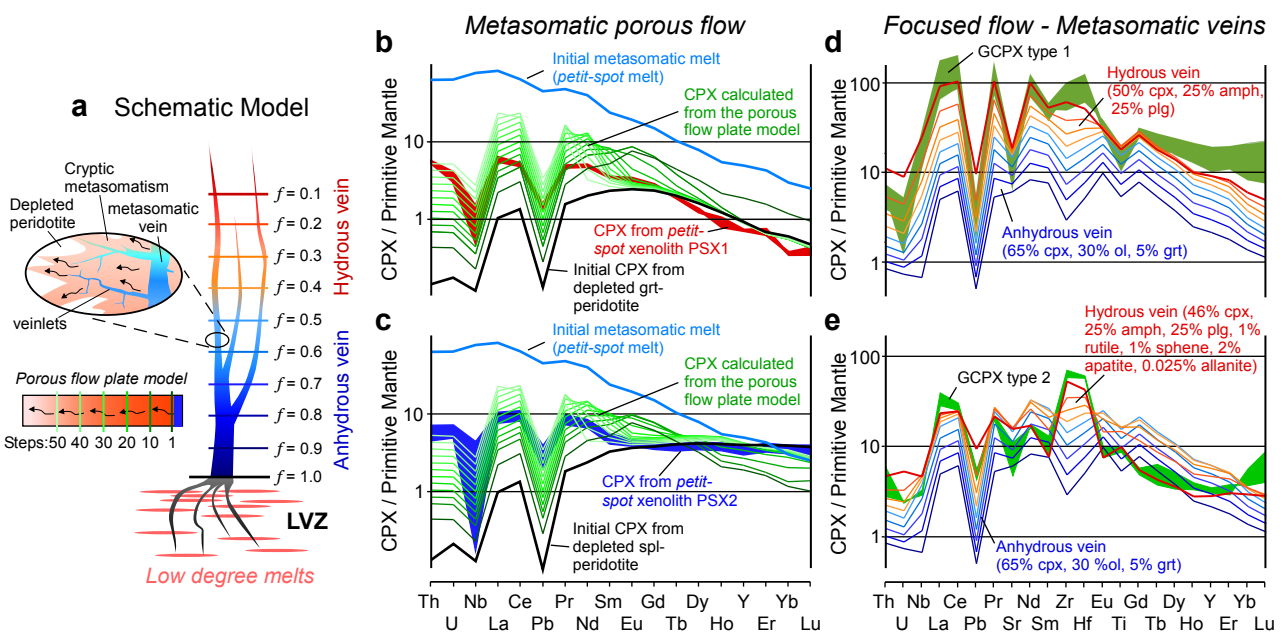
a Schematic Model
Cryptic metasomatism
Depleted peridotite
metasomatic vein
veinlets
Porous flow plate model
Steps:50 40 30 20 10 1
f = 0.1
f = 0.2
f = 0.3
f = 0.4
f = 0.5
f = 0.6
f = 0.7
f = 0.8
f = 0.9
f = 1.0
Hydrous vein
Anhydrous vein
LVZ
Low degree melts
b
Metasomatic porous flow
Initial metasomatic melt (petit-spot melt)
CPX calculated from the porous flow plate model
CPX from petit-spot xenolith PSX1
Initial CPX from depleted grt-peridotite
CPX / Primitive Mantle
c
Initial metasomatic melt (petit-spot melt)
CPX calculated from the porous flow plate model
CPX from petit-spot xenolith PSX2
Initial CPX from depleted spl-peridotite
Th Nb Ce Pr Sm Gd Dy Y Yb
U La Pb Nd Eu Tb Ho Er Lu
d
Focused flow - Metasomatic veins
GCPX type 1
Hydrous vein (50% cpx, 25% amph, 25% plg)
Anhydrous vein (65% cpx, 30% ol, 5% grt)
e
Hydrous vein (46% cpx, 25% amph, 25% plg, 1% rutile, 1% sphene, 2% apatite, 0.025% allanite)
GCPX type 2
Anhydrous vein (65% cpx, 30 %ol, 5% grt)
Th Nb Ce Pr Nd Zr Eu Gd Dy Y Yb
U La Pb Sr Sm Hf Ti Tb Ho Er Lu